

Original article

Usefulness of intraoperative diagnosis of hepatic tumors located at the liver surface and hepatic segmental visualization using indocyanine green-photodynamic eye imaging

5 Takafumi Abo, MD¹, Atsushi Nanashima, MD¹, Syuuichi Tobinaga, MD¹, Shigekazu Hidaka, MD¹, Naota Taura, MD², Katsunori Takagi, MD¹, Junichi Arai, MD¹, Hisamitsu Miyaaki, MD², Hidetaka Shibata, MD², and Takeshi Nagayasu MD¹

*¹Department of Surgical Oncology and ²Department of Gastroenterology and Hepatology,
10 Department of Translational Medical Sciences, Nagasaki University Graduate School of Biomedical Sciences, 1-7-1 Sakamoto, Nagasaki 852-8501, Japan*

Running title: *Utility of ICG-PDE in hepatectomy*

15 The authors have no commercial interests or financial supports to disclose

Address all correspondence to: Atsushi Nanashima, MD

Department of Surgical Oncology, Nagasaki University Graduate School of Biomedical Sciences, 1-7-1 Sakamoto, Nagasaki 852-8501, Japan

Tel.: +81-95-819-7304, Fax: +81-95-819-7306

20 E-mail: a-nanasm@nagasaki-u.ac.jp

ABSTRACT

Background To improve the diagnostic accuracy for hepatic tumors on the liver surface, we investigated the usefulness of an indocyanine green-photodynamic eye (ICG-PDE) system by comparison with Sonazoid intraoperative ultrasonography (IOUS) in 117 patients. Hepatic segmentation by ICG-PDE was also evaluated.

Methods ICG was administered preoperatively for functional testing and images of the tumor were observed during hepatectomy using a PDE camera. ICG was injected into portal veins to determine hepatic segmentation.

Results Accurate diagnosis of liver tumors was achieved with ICG-PDE in 75% of patients, lower than with IOUS (94%). False-positive and false-negative diagnosis rates for ICG-PDE were 24% and 9%, respectively. New small HCCs were detected in 3 patients. The ICG fluorescent pattern in tumors was strong staining in 41%, weak staining in 13%, rim staining in 20% and no staining in 26%. Hepatocellular carcinoma predominantly showed strong staining (61%), while rim staining predominated in cholangiocellular carcinoma (60%) and liver metastasis (55%). Hepatic segmental staining was performed in 28 patients, proving successful in 89%.

Conclusion ICG-PDE is a useful tool for detecting the precise tumor location at the liver surface, identifying new small tumors, and determining liver segmentation for liver resection.

Key words: liver tumor; indocyanine green; photodynamic eye; navigation; hepatectomy

INTRODUCTION

45 Hepatic resection is a useful option in the radical treatment of various liver carcinomas.¹
In the surgical procedure, radical resection without residual tumor is necessary to accomplish
high curative rates.² During hepatectomy, palpation and intraoperative ultrasonography
(IOUS) are essential tools to determine tumor locations and identify small tumors undetected
on preoperative imaging. Enhanced US has recently been applied to examine the vascular
50 flow for detecting liver tumors or tumor morphology.^{3,4} The detection of liver malignancies
by US has improved dramatically with the introduction of microbubble agents. Recent reports
have clarified the utility of IOUS using Sonazoid microbubbles for intraoperative
diagnosis.^{5,6} However, detection of small lesions less than 1 cm in diameter and differential
diagnosis from cirrhotic nodules on the liver surface remains difficult with US.⁷ Other
55 diagnostic modalities are therefore needed to facilitate diagnosis at the liver surface.

 Indocyanine green (ICG) has usually been used to examine hepatic functional reserve.^{8,9}
After intravenous administration, ICG immediately combines with serum protein, and this
combined ICG is specifically taken up by the liver and immediately excreted into bile without
being metabolized.¹⁰ In a normal liver, most ICG dissipates in the blood. ICG has also been
60 applied to detect sentinel lymph nodes in cases of breast carcinoma, with detection using a
new medical imaging system applying an infrared light detector, the ICG-photodynamic eye
(PDE).¹¹ Although near-infrared light cannot be seen with the naked eye, the distribution of
subtle fluorescent materials in tissues can be precisely detected using a detector of
near-infrared radiation, because the ICG accumulated in tissue fluoresces under excitation by
65 light from a laser. Applying this approach to detect ICG fluorescence improves the specificity
of ICG detection compared with dye injection detected on macroscopic observation.¹²
ICG-PDE has also recently been applied to detect liver tumors during hepatectomy.¹³⁻¹⁷ ICG
may remain in or around a liver tumor for a couple of days after administration and the

contrast between liver tumor and liver parenchyma can be marked. Accumulation of ICG
70 might differ between histological types or levels of differentiation.¹³ As anatomical resection
of the liver and post-hepatectomy complications are likely to affect patient survival,¹⁸⁻¹⁹
visualization of the precise segmentation for resection and prevention of complications are
important from an oncological perspective. With intravenous or intrabiliary injection of ICG,
detection of segmental fluorescence, clarification of the biliary anatomy and identification of
75 bile leakage at the transected liver becomes possible.²⁰⁻²² However, the diagnostic accuracy,
limitations and clinical applications of ICG-PDE have yet to be fully clarified. We
hypothesized that ICG-PDE can improve the accuracy of diagnosing liver tumors at the liver
surface and that ICG navigation surgery would be feasible as an alternative to blue-dye
injection, or “tattooing”, for achieving anatomical hepatectomy.²³ Accurate diagnosis of
80 tumor location and adequate segmentectomy during surgery are important for achieving
complete cure.

The aim of the present preliminary study was thus to clarify various aspects of ICG-PDE
imaging. For this purpose, we assessed the use of ICG-PDE in 117 patients with benign or
malignant hepatobiliary diseases who underwent surgical resections by comparison with the
85 conventional diagnostic tool of Sonazoid-IOUS, and examined the feasibility and limitations
of this modality for tumor diagnosis. The possibility of applying ICG navigation to
hepatectomy was also considered.

90 **Patients and methods**

Patient background

Study participants comprised 117 patients with hepatobiliary tumors who were scheduled for surgery and admitted to the Division of Surgical Oncology at Nagasaki University Hospital (NUH) between November 2009 and January 2014. In this study, all patients were
95 also examined by Sonazoid-IIOUS as a reference since 2009 after its approval by the Japanese health authorities. Liver tumors included hepatocellular carcinoma (HCC) in 56 patients, intrahepatic cholangiocarcinoma (CCC) in 12, colorectal liver metastasis in 36, hilar bile duct carcinoma in two, gall bladder carcinoma in four, neuroendocrine tumor in one and benign
100 liver tumors in six (including hemangioma in two, angiomyolipoma in one, biliary adenoma in one, liver fibrosis in one and hematoma in one). Patients comprised 79 men and 38 women, with a mean (\pm standard deviation (SD)) age at the time of surgery of 68.6 ± 11.6 years (range, 31-85 years). Background liver disease included normal liver in 42 patients, fatty liver in seven, cancer chemotherapy-associated liver dysfunction in 11, chronic viral hepatitis in 40, cirrhosis due to viral hepatitis in 15 and obstructive jaundice in two. Operative procedures
105 included trisectionectomy, hemihepatectomy or central bisegmentectomy in 31 patients, segmentectomy or sectionectomy in 47, limited resection in 38 and other surgery in two (including tumor biopsy in both cases). All study protocols were approved by the Human Ethics Review Board at our institution. Informed consent for data collection was obtained from each patient during this period. Anesthesia data and patient data were retrieved from the
110 NUH database.

Procedure of Sonazoid-IIOUS and ICG-PDE

Examination of IIOUS and contrast-enhanced IIOUS was performed using a XarioTM XG system (Toshiba Medical Systems, Tokyo, Japan) and a microconvex probe (PVT-375BT, 3.5

115 MHz; Toshiba Medical Systems), as well as an intraoperative probe (PLT-705BTH, 7.5 MHz). All IOUS was performed by surgeons to help determine the need for hepatectomy. For tumors located at the liver surface, the liver was covered with warm saline to reduce the air gap between the probe and liver surface. An intravenous bolus injection of 0.5 ml of perflubutane microbubbles (Sonazoid) was administered via the peripheral vein at the time of making the
120 laparotomy incision to observe Kupffer-phase images at 1-2 h after injection, because the microbubbles remain for a long time.^{5,6} Liver tumors were identified as low-contrast perfusion defects compared with normal liver parenchyma. Intraoperatively, viewing of the late Kupffer-phase images was first started and main liver tumors were clearly detected as perfusion defects, appearing as ill-defined low-echoic areas. Intratumor revascularization in
125 the arterial phase was then examined and poor vascularization was confirmed by the reperfusion technique.

ICG was intravenously injected 4-7 days before hepatectomy to examine the routine ICG retention rate at 15 min, in order to evaluate hepatic functional reserve, as a necessary step in deciding on operative indications.^{8,9} When ICG testing was performed over 14 days
130 before hepatectomy, 10 ml of diluted ICG (0.5 mg/kg of ICG dissolved in distilled water) was intravenously injected the day before hepatectomy. During laparotomy, under dark conditions, a PDE camera system (Hamamatsu Photonics, Hamamatsu, Japan) (Fig. 1) was applied to detect ICG fluorescence. This system irradiated the ICG combined with serum protein with infrared light (wavelength, 750-830 nm). The excited ICG fluoresced at a wavelength of 845
135 nm, which was detected by the PDE detector. First, to determine tumor location, the surface of the whole liver was observed. All liver tumors and lesions newly detected by ICG-PDE were also observed by palpation and Sonazoid-IOUS again.⁵ Small spots of strong fluorescence less than 5 mm in diameter identified by ICG-PDE were partially resected as biopsy specimens in the present study (Fig. 2A). The pattern of fluorescent on ICG-PDE for

140 liver tumors was defined as: 1) strong stain (Fig. 2B); 2) weak stain (Fig. 2C); 3) rim stain
around the tumor (Fig. 2D); or 4) no stain. In this study, a false-positive result was defined as
positive fluorescence on ICG-PDE of a non-tumorous lesion, and a false-negative result was
defined as no fluorescence on ICG-PDE of a tumorous lesion.

Subsequently, in cases requiring anatomical hepatic resection, 5 ml of ICG diluted with
145 100 ml of distilled water (0.25 mg/ml) was intraoperatively injected into the portal vein
supplying the estimated area for liver resection under IOUS. Accompanied by macroscopic
findings for ICG dye and IOUS, the area of fluorescing liver was marked by diathermy (Fig.
3A). After hepatic resection, resected tumors and surgical margins were observed for
specimens and the amputated area of remnant liver. To detect bile duct leakage at the cut
150 surface, 0.25 mg/ml of ICG was injected into the bile duct via the cystic duct and careful
examination for tiny spots or extravasation of bile was performed at the cut surface (Fig. 3B).

Statistical analysis

All continuous data are expressed as mean \pm SD. Data were compared between groups using
155 one-way analysis of variance (ANOVA). The chi-square test was used to compare categorical
variables. Two-tailed P values <0.05 were considered significant. SPSS for Windows version
18.0 software (SPSS, an IBM Company, Chicago, IL) was used for all statistical analyses.

160 **Results**

Feasibility and diagnosis of liver tumors by ICG-PDE

Intraoperative ICG-PDE was able to be carried out for all patients without ICG-related side effects. Mean tumor size was 3.6 ± 1.8 cm (range, 0.5-8.5 cm). Accurate diagnosis of benign and malignant liver tumors was achieved in 110 of 117 patients (94%) by Sonazoid-IOUS and 88 of 117 patients (75%) by ICG-PDE. A difference in diagnosis was seen between 165 Sonazoid-IOUS and ICG-PDE in 27 of the 117 patients (24%). No significant relationship between tumor location and detectability of ICG-PDE was observed (data not shown). False-positive and false-negative diagnoses by Sonazoid-IOUS numbered three (2%) and seven (6%), while those by ICG-PDE numbered 28 (24%) and 10 (9%), respectively. Reasons 170 for lesions being technically undetectable on ICG-PDE included depth of the tumor (fluorescence was not observed in deep lesions >10 mm from the liver surface due to the limitations of fluorescent permeability) in seven patients (5.6%).

Diagnostic accuracy for malignant liver tumor in the 117 patients was compared between Sonazoid-IOUS and ICG-PDE. Sonazoid-IOUS diagnosed 109 of 111 malignant tumors and 175 5 of 6 non-malignant tumors. Sensitivity, specificity, positive predictive value, negative predictive value and accuracy were 98%, 83%, 99%, 71% and 97%, respectively. ICG-PDE diagnosed 85 of 111 malignant tumors and 3 of 6 non-malignant tumors. Sensitivity, specificity, positive predictive value, negative predictive value and accuracy were 77%, 50%, 97%, 10% and 75%, respectively. Single diagnostic accuracy for malignant liver tumors was 180 higher for Sonazoid-IOUS than for ICG-PDE.

The ICG fluorescent pattern in liver tumors was divided into four types, as follows: strong staining in 47 patients (41%); weak staining in 15 (13%); rim staining surrounding the tumor in 25 (20%); and no staining in 30 (26%). The relationship between the ICG fluorescent pattern of the tumor lesion and the type of liver tumor is shown in Table 1.

185 In benign tumors, angiomyolipoma with hypervascular enhancement showed strong ICG staining, while biliary adenoma with mild vascularity showed weak homogeneous staining. Cavernous hemangioma showed rim staining. Non-tumorous lesions showed no staining. All benign lesions were able to be diagnosed by ICG-PDE.

In malignant tumors, ICG fluorescence was observed in 41 of 56 patients (74%) with
190 HCC; strong staining was predominantly observed in these cases, representing 61%. Rim staining was observed in only one patient. ICG fluorescence was observed in 10 of 12 patients (83%) with CCC; for these cases, rim staining was predominantly observed, representing 60%. Strong staining was observed in 30%. ICG fluorescence was observed in 31 of the 36 patients (86%) with liver metastasis; these patients predominantly showed rim
195 staining, representing 55%. Strong or weak staining was observed in 47%. One patient with neuroendocrine liver tumor with hypervascularity showed strong staining. In the gallbladder, one patient with liver bed invasion showed strong staining, but three other tumors did not show any staining. The two patients with bile duct carcinoma showed no staining without liver metastasis.

200 ICG-PDE fluorescent patterns for accessory benign liver lesions in patients with malignant tumors are shown in Table 2. Liver cysts showed ICG fluorescence in 7 of 12 lesions (58%), while small hemangioma showed fluorescence in 4 of 6 lesions (67%). Small spot fluorescence was observed in seven lesions and an ablated lesion showed rim staining. In cirrhotic liver, weaker, non-specific staining was seen in comparison with the fluorescence
205 detectable in main tumors, possibly due to a delayed discharge of ICG into liver parenchyma. Bile leakage spot was observed in two cases (Fig. 2B). New small lesions of intrahepatic metastasis from the main HCC apparent only on ICG-PDE were observed in three patients. On the other hand, intrahepatic metastasis from the main HCC was not detected by ICG-PDE in four patients. Three patients showed visible tumor lesions between 5 and 8 mm in diameter.

210 A non-visible lesion 2 mm in diameter was histologically confirmed in the resected specimen
from one patient. Strong fluorescence of macroscopic tumor thrombus in the portal trunk was
achieved via the portal vein wall in two patients. Lymph node metastasis of CCC was not
detected by ICG-PDE.

215 **Segmental visualization by fluorescent staining using ICG-PDE**

Hepatic segmental or sectional staining for ICG-PDE navigation hepatectomy was performed
for 28 patients. The scheduled segmental staining could be performed in 25 patients (89%)
for whom a burden of the posterior sector and caudate lobe could be counter-stained (the
posterior sector was stained and the caudate lobe was not). The remaining three patients
220 showed technical failure of scheduled segmental staining including caudate counter-staining.

Discussion

ICG-PDE has recently been applied to detect lymph nodes via the lymphatic duct in the fields
225 of breast and digestive surgery,^{11,24,25} and to detect vascular flow in other fields of
surgery.^{12,26,27} The PDE system is thus useful to observe the dynamic changes of various
materials inside the body. In the hepato-biliary-pancreatic field, application of ICG-PDE has
also been attempted to detect the intrahepatic tumor location, hepatic segmentation, biliary
leakage and status for biliary surgery.^{13-22,28} However, to the best of our knowledge, the
230 usefulness and reliability of ICG-PDE in this field have not been fully clarified. From
previous reports, the depth of tissue detectable by ICG-PDE might be less than 10 mm (no
data or references shown), so this diagnosis may be applicable only at the liver surface or on
cut surfaces of hepatic parenchyma. ICG that has combined with serum protein in the liver
usually washes out within several hours, but remains trapped for a long period within liver
235 tumors such as HCC, ICC, and metastatic liver carcinomas.¹³⁻²² In the case of ICG testing,
ICG is specifically collected in the liver via hepatic blood flow and the hypervascular liver
area shows marked staining. ICG is then metabolized in the hepatic cells and immediately
excreted into bile. However, in hypervascular tumor lesions, ICG is trapped and excretion
may be delayed for a long period. However, the mechanisms underlying retention in
240 malignancies have not yet been clarified, although ICG might be trapped in cancer cells in
cases of hypervascular tumors such as HCC.¹³ This type of lesion could thus be detected
using a near-infrared ray detector in the ICG-PDE system.¹²

Alternatively, Sonazoid-IOUS offers a powerful approach for imaging diagnosis to detect
tumor distributions.⁵⁻⁷ Sonazoid became available as a contrast medium containing
245 microbubbles in 2007, and has been widely applied for the diagnosis of liver tumors
including HCC, CCC and liver metastasis.^{5-7,15,22} The introduction of this agent has markedly
improved the accuracy of diagnosing liver tumors to levels similar to those of magnetic

resonance imaging with gadolinium ethoxybenzyl diethylenetriaminepentaacetic acid.²⁹

Although even small lesions could be detected in deep areas of the liver by Sonazoid-IOUS, detection at the liver surface or on cut surfaces represent a blind spot for this approach.⁵ This modality has already been established as the conventional diagnostic tool at our institute. We therefore hypothesized that the combination of Sonazoid-IOUS and ICG-PDE would offer a more powerful diagnostic tool for the intraoperative detection of tumor distribution. However, the advantages and limitations of each modality should also be clarified.

In the present series, all liver tumors could be detected by ICG-PDE. In 117 patients, we attempted both Sonazoid-US and ICG-PDE during hepatectomy to overcome the limitation of Sonazoid-IOUS alone. Occult metastatic lesions undetected on preoperative examinations and IOUS were expected to be detected by the new powerful diagnostic tool according to the hypothesis of the present study. As a result, the overall rate of accurate diagnosis by ICG-PDE was lower than that by Sonazoid-IOUS, because of the different fluorescent rates in various tumors, tumor depth, and the limited size of small tumors. Occult intrahepatic metastasis could be observed in only three patients and the clinical significance of additional ICG-PDE was very limited. With respect to the accurate diagnosis of malignant liver tumors, Sonazoid-IOUS was more reliable and available as the conventional diagnostic tool during hepatectomy according to our results. However, the aim of the present study was to clarify the diagnostic limitations of IOUS of the liver surface combined with ICG-PDE. From this perspective, our concept of a combination method might be useful in improving surgical results.

According to recent reports, the fluorescent patterns of liver tumors vary among homogeneous strong staining, heterogeneous weak staining, staining surrounding the tumor or no staining.¹⁵⁻¹⁷ Such variation was confirmed in the present series. In hypervascular benign tumors, ICG fluorescence was strongly detected due to vascular retention. However,

in the non-structural area of nodular lesions, no fluorescence was observed. ICG-PDE might thus be useful for differentiation from non-tumorous lesions in the liver. Among the malignant lesions, hypervascular tumors such as HCC, some CCC and neuroendocrine tumors showed strong staining by ICG retention. In cases of liver tumor with strong fluorescence, residual tumor lesions at the resected edge were easily observed and some additional lesions could be completely resected. Among colorectal liver metastasis, vascularity was often observed around the tumor, so detecting the edge of the surgical margins might be difficult for colorectal tumors. We attempted ICG-PDE for adjacent malignancies, such as gallbladder carcinoma or bile duct carcinoma. However, ICG-PDE is not useful for detecting fluorescence of the main tumor or surrounding cancer metastasis, because of the low rate of fluorescence. Among accessory lesions, cysts and hemangiomas were identifiable from ICG-PDE, so a false-positive diagnosis must be ruled out. In benign cysts, fluorescence of ICG was caused by fluid retained in the cyst, but not by hemorrhage, and the precise mechanisms underlying this phenomenon have yet to be explained. In such accessory lesions with identification of biliary leakage spots and detection of portal vein thrombosis, the clinical usefulness of ICG-PDE has already been reported.¹⁷⁻²²

In patients with severe liver injury such as cirrhosis or those who underwent ICG administration within a few days, multiple false-positive fluorescent spots were observed. False-positive spots have also been previously reported observed in tumor diagnosis.¹⁶ This problem remains in patients with very poor liver function who may have undergone liver transplantation,³⁰ but few problems of false-positive areas were seen in patients indicated for hepatectomy in the present study. As shown from our results, false-positive areas were shown as tiny spots that were readily distinguished from true liver lesions. Some patients occasionally undergo ablation therapy or transarterial chemoembolization (TACE) prior to the hepatectomy. This results in alteration of the echogenicity of the treated area, appearing

as hypoechoic lesions. Accurate differentiation between necrotic lesions and viable tumors may then be difficult by conventional US. However, early vascularization in the tumor area or surrounding region is a sign of tumor viability.³¹ In the resected area after hepatectomy, subtle remnant tumor cannot be macroscopically observed intraoperatively. The cut surface under ICG-PDE showed spotted areas of remnant tumor confirmed by histological findings in some of our cases.

Anatomical resection of the liver can be needed under various circumstances, as described above.¹⁸ Another application of ICG-PDE is segmentation by portal injection of ICG.¹⁸⁻²² Tattooing or blue-dye segmentation has been applied to achieve anatomical segmentectomy or sectorectomy.²³ With those methods, visualization of the stained area is sometimes difficult and the dye soon washes out. Segmentation using ICG-PDE might enable clearer detection, although detailed comparisons were not performed in the present study. The usefulness of ICG-PDE segmentation compared with the conventional dye method has also not yet been reported. The present series also applied ICG-PDE segmentation as a counter-stain for non-stained areas to confirm the segment to be resected in the caudate lobe or segment 8. By injecting ICG into the bile duct, biliary fistula could be sensitively detected using the ICG-PDE system, as described in previous reports.^{18,28} In the present series, unexpected areas of biliary fistula could be detected by testing for bile leakage just after hepatectomy in a few cases. In one patient who underwent right hepatectomy, amputated-type biliary fistula in the remnant left caudate lobe that could not be controlled by chemical ablation or fibrin glue was able to be detected by ICG-PDE during reoperation for fixation of biliary fistula. This lesion was locally ablated and well-controlled after reoperation.

Future applications of ICG-PDE have recently been proposed. One approach is application to tumor detection during laparoscopic hepatectomy.³² Development of a laparoscopy-exclusive ICG-PDE system is expected. Another application is use in photodynamic therapy (PDT) to

treat ICG-accumulating liver tumors by laser excitation using light of different wavelengths.³³

At present, although sufficient effects of PDT using ICG-PDE have not been confirmed, a

325

recent report by Kaneko et al. showed the possibility of PDT with ICG-PDE for liver cancer

in an animal model.³⁴ Such a laser-applied tools could be improved for future approaches. In

conclusion, we have demonstrated that ICG-PDE allows easy examination of the tumor

distribution, including identification of new lesions or remnant cancer at the liver surface or

cut edge after hepatectomy, for detection of the extent of portal trunk tumor thrombosis of

330

HCC, for detection of unexpected biliary fistula, and for determination of the extent of the

area to be resected by portal vein injection as a method of ICG navigation, potentially

facilitating decision-making for hepatic resection. This new imaging modality could become

a standard procedure combined with enhanced IOUS or palpation in patients with liver

tumors who undergo hepatectomy.

335

Conflict of interest statement

The authors declare that they have no conflicts of interest.

340 **REFERENCES**

1. Song TJ, Ip EW, Fong Y. Hepatocellular carcinoma: current surgical management. *Gastroenterology* 2004;127:S248-260.
2. Altendorf-Hofmann A, Scheele J. A critical review of the major indicators of prognosis after resection of hepatic metastases from colorectal carcinoma. *Surg Oncol Clin N Am* 2003;12:165-192
3. Torzilli G, Makuuchi M. Intraoperative ultrasonography in liver cancer. *Surg Oncol Clin N Am* 2003;12:91-103.
4. Poon RT. Recent advances in techniques of liver resection. *Surg Technol Int* 2004;13:71-77.
- 350 5. Nanashima A1, Tobinaga S, Abo T, et al. Usefulness of sonazoid-ultrasonography during hepatectomy in patients with liver tumors: A preliminary study. *J Surg Oncol.* 2011;103:152-157.
6. Nakano H, Ishida Y, Hatakeyama T, et al. Contrast-enhanced intraoperative ultrasonography equipped with late Kupffer-phase image obtained by sonazoid in
- 355 patients with colorectal liver metastases. *World J Gastroenterol.* 2008;14:3207-3211.
7. Numata K, Morimoto M, Ogura T, et al. Ablation therapy guided by contrast-enhanced sonography with Sonazoid for hepatocellular carcinoma lesions not detected by conventional sonography. *J Ultrasound Med* 2008;27:395-406.
8. Takasaki T, Kobayashi S, Suzuki S, et al. Predetermining postoperative hepatic function
- 360 for hepatectomies. *Int. Surg.* 1980;65:309-313
9. Kubota K, Makuuchi M, Kusaka K, et al. Measurement of liver volume and hepatic functional reserve as a guide to decision-making in resection surgery for hepatic tumors. *Hepatology* 1997;26:1176-1181.

10. Wilson SA, Tavendale R, Hewick DS. The biliary elimination of amaranth, indocyanine
365 green and nitrazepam in germ-free rats. *Biochem Pharmacol.* 1985;34:857-863.
11. Hojo T, Nagao T, Kikuyama M, et al. Evaluation of sentinel node biopsy by combined
fluorescent and dye method and lymph flow for breast cancer. *Breast.* 2010;19:210-213.
12. Unno N, Suzuki M, Yamamoto N, et al. Indocyanine green fluorescence angiography for
intraoperative assessment of blood flow: a feasibility study. *Eur J Vasc Endovasc Surg.*
370 2008;35:205-7.
13. Gotoh K, Yamada T, Ishikawa O, et al. A novel image-guided surgery of hepatocellular
carcinoma by indocyanine green fluorescence imaging navigation. *J Surg Oncol.*
2009;100:75-79.
14. Uchiyama K, Ueno M, Ozawa S, et al. Combined use of contrast-enhanced intraoperative
375 ultrasonography and a fluorescence navigation system for identifying hepatic metastases.
World J Surg. 2010;34:2953-2959.
15. Kasuya K, Sugimoto K, Kyo B, et al. Ultrasonography-guided hepatic tumor resection
using a real-time virtual sonography with indocyanine green navigation (with videos). *J
Hepatobiliary Pancreat Sci.* 2011;18:380-385.
- 380 16. Ishizuka M, Kubota K, Kita J, et al. Intraoperative observation using a fluorescence
imaging instrument during hepatic resection for liver metastasis from colorectal cancer.
Hepatogastroenterology. 2012;59:90-2.
- 17 Peloso A, Franchi E, Canepa MC, et al. Combined use of intraoperative ultrasound and
indocyanine green fluorescence imaging to detect liver metastases from colorectal cancer.
385 *HPB (Oxford).* 2013;15:928-34.
- 18 Eguchi S, Kanematsu T, Aarii S, et al.; Liver Cancer Study Group of Japan. Comparison of
the outcomes between an anatomical subsegmentectomy and a non-anatomical minor

- hepatectomy for single hepatocellular carcinomas based on a Japanese nationwide survey. *Surgery*. 2008;143:469-75.
- 390 19 Nanashima A1, Abo T, Hamasaki K, et al. Perioperative non-tumorous factors associated with survival in HCC patients who underwent hepatectomy. *Anticancer Res*. 2011;31:4545-51.
20. Kaibori M, Ishizaki M, Matsui K, et al. Intraoperative indocyanine green fluorescent imaging for prevention of bile leakage after hepatic resection. *Surgery*. 2011;150:91-98.
- 395 21. Aoki T, Yasuda D, Shimizu Y, et al. Image-guided liver mapping using fluorescence navigation system with indocyanine green for anatomical hepatic resection. *World J Surg*. 2008;32:1763-1767.
22. Uchiyama K, Ueno M, Ozawa S, et al. Combined intraoperative use of contrast-enhanced ultrasonography imaging using a sonazoid and fluorescence navigation system with
400 indocyanine green during anatomical hepatectomy. *Langenbecks Arch Surg*. 2011;396:1101-1107.
23. Takayama T, Makuuchi M, Watanabe K, et al. A new method for mapping hepatic subsegment: counterstaining identification technique. *Surgery*. 1991;109:226-9.
24. Noura S, Ohue M, Seki Y, et al. Feasibility of a lateral region sentinel node biopsy of
405 lower rectal cancer guided by indocyanine green using a near-infrared camera system. *Ann Surg Oncol*. 2010;17:144-151.
25. Miyashiro I, Hiratsuka M, Kishi K, et al. Intraoperative diagnosis using sentinel node biopsy with indocyanine green dye in gastric cancer surgery: an institutional trial by experienced surgeons. *Ann Surg Oncol*. 2013;20:542-546.
- 410 26. Okusanya OT1, Madajewski B, Segal E, et al. small portable interchangeable imager of fluorescence for fluorescence guided surgery and research. *Technol Cancer Res Treat*. 2013. [Epub ahead of print]

27. Buretta KJ, Brat GA, Christensen JM, et al. Near-infrared lymphography as a minimally
invasive modality for imaging lymphatic reconstitution in a rat orthotopic hind limb
415 transplantation model. *Transpl Int.* 2013;26:928-937.
28. Spinoglio G, Priora F, Bianchi PP, et al. Real-time near-infrared (NIR) fluorescent
cholangiography in single-site robotic cholecystectomy (SSRC): a single-institutional
prospective study. *Surg Endosc.* 2013;27:2156-2162.
29. Kudo M, Matsui O, Sakamoto M, et al. Role of gadolinium- ethoxybenzyl-
420 diethylenetriamine pentaacetic acid-enhanced magnetic resonance imaging in the
management of hepatocellular carcinoma: consensus at the Symposium of the 48th
Annual Meeting of the Liver Cancer Study Group of Japan. *Oncology.* 2013;84:21-27.
30. Tanaka T, Takatsuki M, Hidaka M, et al. Is a fluorescence navigation system with
indocyanine green effective enough to detect liver malignancies? *J Hepatobiliary*
425 *Pancreat Sci.* 2013 doi: 10.1002/jhbp.17. [Epub ahead of print]
31. Muramatsu Y, Takayasu K, Moriyama N, et al. Peripheral low-density area of hepatic
tumors: CT-pathologic correlation. *Radiology.* 1986;160:49-52.
32. van der Pas MH, Ankersmit M, Stockmann HB, et al. Laparoscopic sentinel lymph node
identification in patients with colon carcinoma using a near-infrared dye: description of a
430 new technique and feasibility study. *J Laparoendosc Adv Surg Tech A.* 2013;23:367-371.
33. Wang JD, Shen J, Zhou XP, et al. Optimal treatment opportunity for mTHPC-mediated
photodynamic therapy of liver cancer. *Lasers Med Sci.* 2013;28:1541-1548.
34. Kaneko J, Inagaki Y, Ishizawa T, et al. Photodynamic therapy for human
hepatoma-cell-line tumors utilizing biliary excretion properties of indocyanine green. *J*
435 *Gastroenterol.* 2014;49:110-116.

FIGURE LEGENDS

Fig. 1 The ICG-PDE camera system.

440 **Fig. 2** Representative image of the ICG-PDE system during operation. A small (less than 5 mm in diameter), strongly fluorescing spot on ICG-PDE (A). The pattern of ICG-PDE fluorescence in liver tumors was defined as: 1) strong stain (B); 2) weak stain (C); 3) rim staining around the tumor (D); or 4) no stain. B and C show sections from a resected specimen.

445

Fig. 3 Findings of ICG dye injection in the portal vein for the targeted segment. The fluorescing area of liver (segments 7 and 8) show marked ICG fluorescence (A). To detect bile duct leakage by ICG injection into the bile duct, tiny spots or extravasation of bile were confirmed as strongly fluorescing spot lesions on the cut surface (B).

450

Fig. 1



Fig. 2

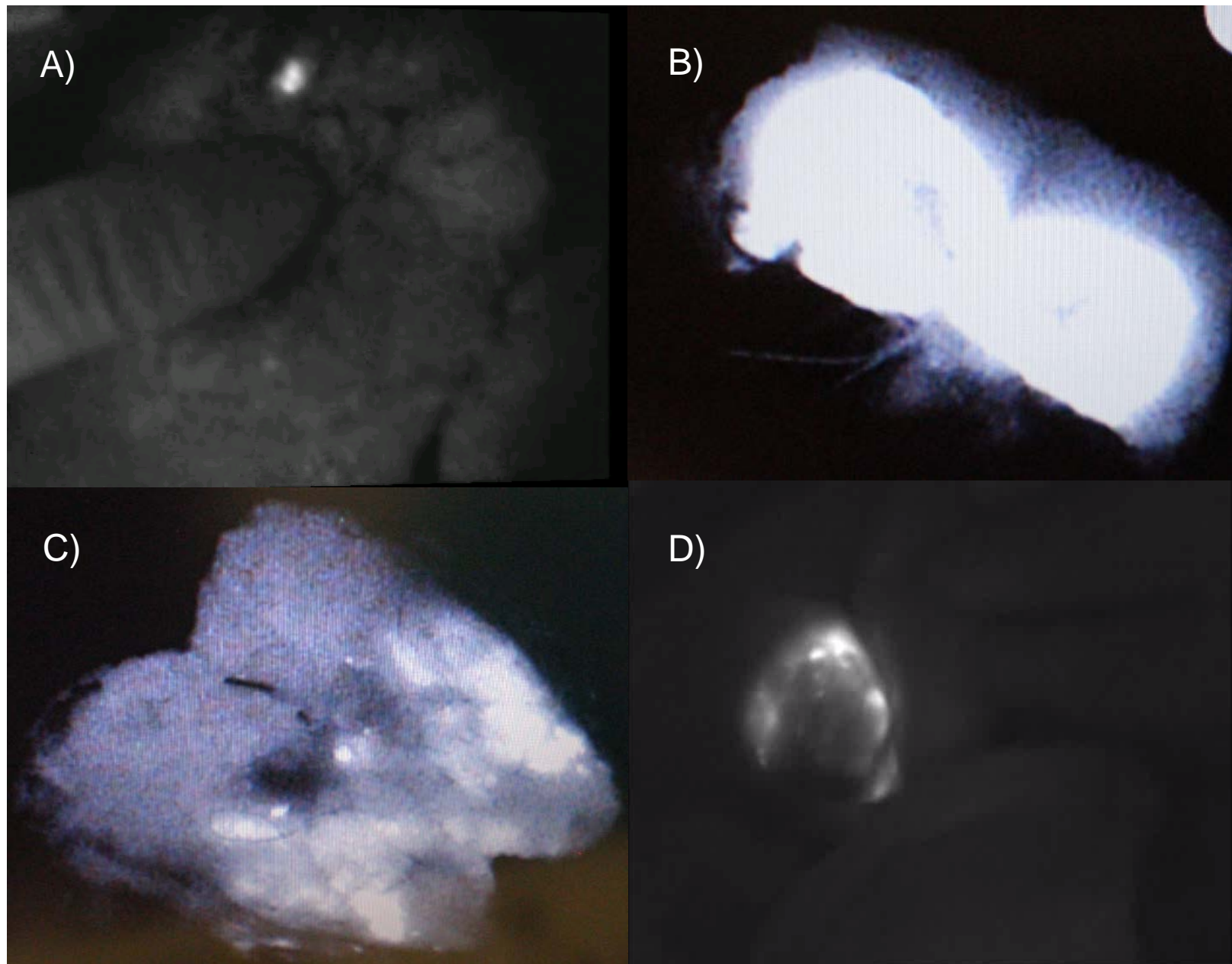
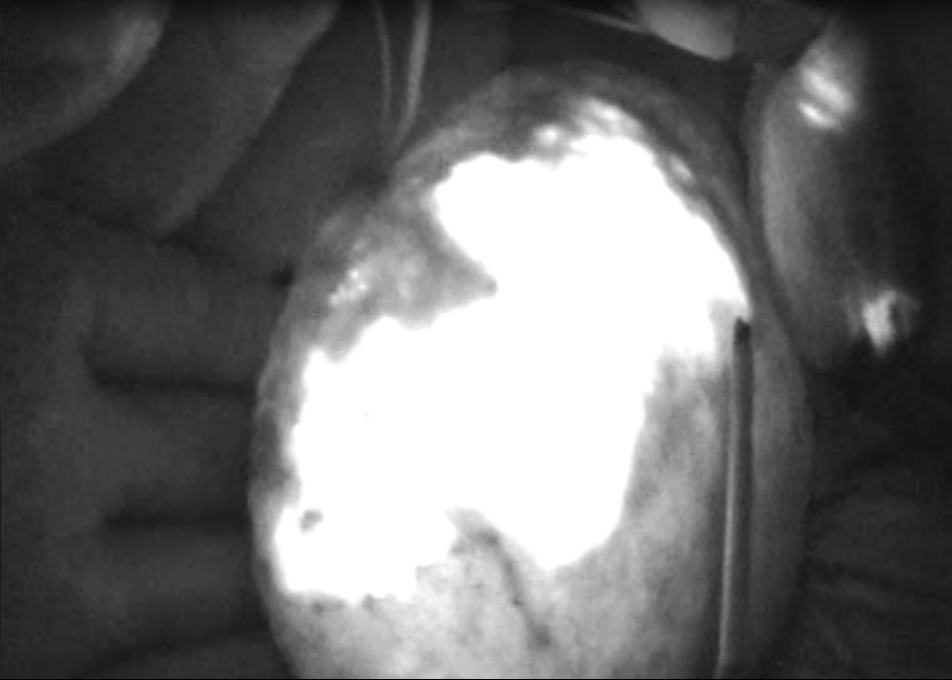


Fig. 3

A)



B)

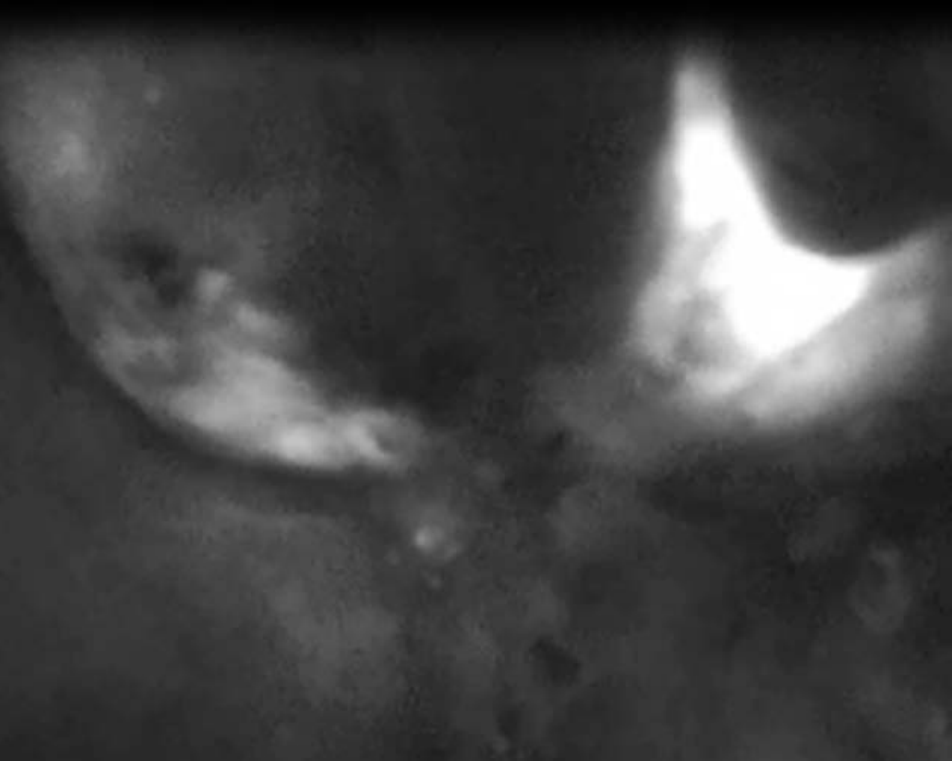


TABLE 1. ICG fluorescent pattern and main liver tumor by ICG-PDE

	Strong stain (n=47)	Weak stain (n=15)	Rim stain (n=25)	No stain (n=30)
Benign tumor				
Angiomyolipoma	1			
Biliary adenoma		1		
Cavernous hemangioma			1	
Non-tumor lesion				
Local fibrosis				1
Organizing hematoma				1
Malignant tumor				
Hepatocellular carcinoma	34	6	1	15
Cholangiocellular carcinoma	3	1	6	2
Colorectal liver metastasis	7	7	17	5
Neuroendocrine tumor	1			
Gallbladder carcinoma*	1			3
No liver metastasis				
Bile duct carcinomas				2

* One patient with liver bed invasion

5 **TABLE 2. ICG fluorescent pattern and accessory liver tumors by ICG-PDE**

	Strong stain (n=26)	No stain (n=12)
Benign tumor		
Simple cyst	7	5
Small hemangioma	4	2
Non-tumor lesion		
Cirrhotic small nodule	6	
Ablated lesion	1*	
Bile leakage at resected area	2	
Malignant tumor		
Intrahepatic metastasis of HCC	3	4
Portal trunk thrombosis of HCC	2	0
Adrenal gland metastasis of HCC	1	
Node metastasis of CCC		1

* Rim stain